AD-A143 695 AERODYNAMIC FEASIBILITY FOR AIRBORNE RETRIEVAL OF A REMOTELY PILOTED VEHICLE(U) DAVID W TAYLOR NAVAL SHIP RESEARCH AND DEVELOPMENT CENTER BET.. 1/1

UNCLASSIFIED E F MCCABE ET AL. NOV 76 DTNSRDC-76/0043 F/G 1/2 NL

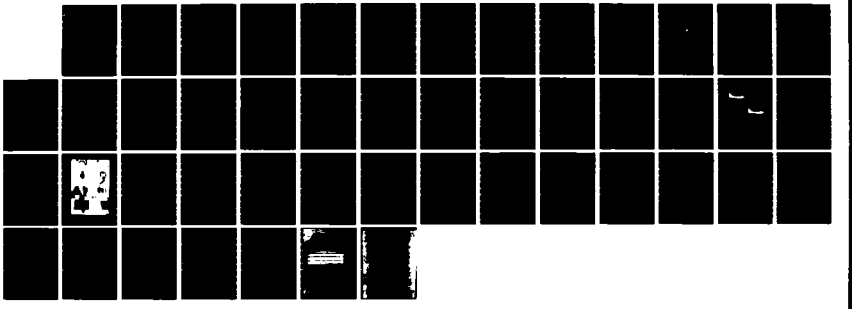

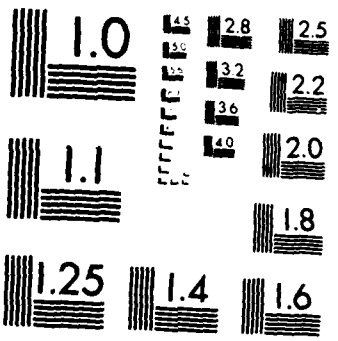

DAVID W. TAYLOR NAVAL SHIP RESEARCH AND DEVELOPMENT CENTER

Bethesda, Md. 20084

AERODYNAMIC FEASIBILITY FOR AIRBORNE RETRIEVAL OF A REMOTELY PILOTED VEHICLE

by

Earl F. McCabe, Jr. and David W. Lacey

AVIATION AND SURFACE EFFECTS DEPARTMENT
RESEARCH AND DEVELOPMENT REPORT

November 1976

Report 76-0043

AERODYNAMIC FEASIBILITY FOR AIRBORNE RETRIEVAL OF A REMOTELY PILOTED VEHICLE Report 76-0043

MAJOR DTNSRDC ORGANIZATIONAL COMPONENTS

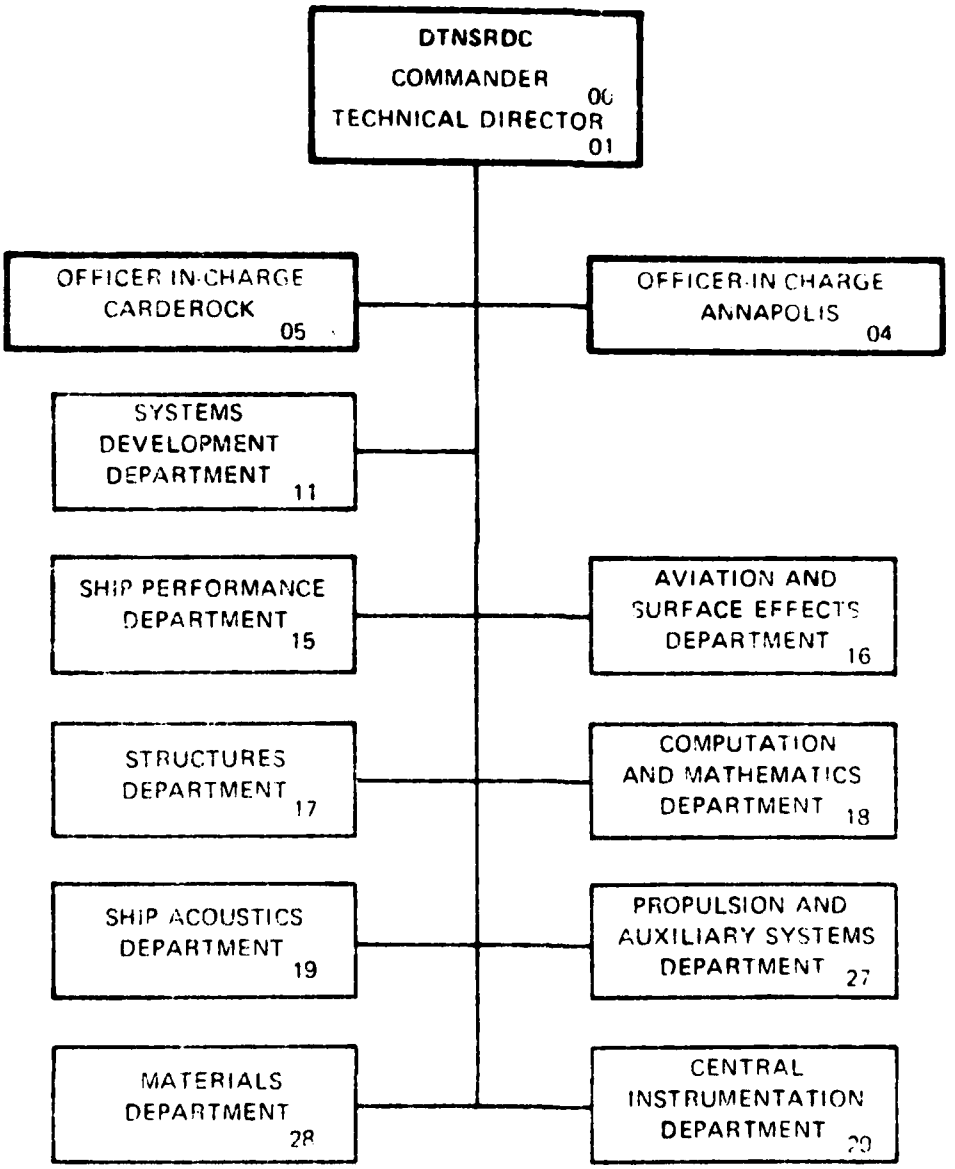

UNCLASSIFIED

SECURITY CLASSIFICATION OF THIS PAGE (When Data Entered)

REPORT DOCUMENTATION PAGE	READ INSTRUCTIONS BEFORE COMPLETING FORM
1 REPORT NUMBER: 76-0043	2 GOVT ACCESSION NO: AD-A034 3695
3 RECIPIENT'S CATALOG NUMBER	
4 TITLE (and Subtitle): AERODYNAMIC FEASIBILITY FOR AIRBORNE RETRIEVAL OF A REMOTELY PILOTED VEHICLE	5 TYPE OF REPORT & PERIOD COVERED: Final
	6 PERFORMING ORG. REPORT NUMBER
7 AUTHOR(s): Earl F. McCabe, Jr. and David W. Lacey	8 CONTRACT OR GRANT NUMBER(s)
9 PERFORMING ORGANIZATION NAME AND ADDRESS: David W. Taylor Naval Ship Research and Development Center, Bethesda, Maryland 20084	10 PROGRAM ELEMENT, PROJECT, TASK AREA & WORK UNIT NUMBERS: Program Element 63796N, Task Area W3359, Work Unit 1660-253
11 CONTROLLING OFFICE NAME AND ADDRESS: Commander, Naval Air Systems Command (PMA 247), Washington, D.C. 20631	12 REPORT DATE: NOVEMBER 1976
	13 NUMBER OF PAGES: 43
14 MONITORING AGENCY NAME & ADDRESS (if different from Controlling Office)	15 SECURITY CLASS. (of this report): UNCLASSIFIED
	15a DECLASSIFICATION DOWNGRADING SCHEDULE

16 DISTRIBUTION STATEMENT (of this Report)

APPROVED FOR PUBLIC RELEASE: DISTRIBUTION UNLIMITED

17 DISTRIBUTION STATEMENT (of the abstract entered in Block 20, if different from Report)

18 SUPPLEMENTARY NOTES

19 KEY WORDS (Continue on reverse side if necessary and identify by block number)

A-7
Aircraft
Airborne Retrieval
Captive Trajectory System
Remotely Piloted Vehicle
Stability and Control

20 ABSTRACT (Continue on reverse side if necessary and identify by block number)

A combined wind tunnel/computer analysis was undertaken to evaluate the aerodynamic feasibility for airborne recovery of a fixed-wing remotely piloted vehicle (RPV). A map of aerodynamic loads interacting on the aircraft and RPV was obtained in the wind tunnel. The flow field was then represented mathematically and used to evaluate the aerodynamic feasibility of airborne retrieval. It was concluded that retrieval forward of the aircraft is potentially dangerous, unless a separation of more than two meters is

DD FORM 1 JAN 73 1473 EDITION OF 1 NOV 65 IS OBSOLETE
S/N 0102-014-6601

UNCLASSIFIED

SECURITY CLASSIFICATION OF THIS PAGE (When Data Entered)

maintained; retrieval aft of the aircraft is aerodynamically safe without restriction. In addition, it was determined that the primary effect of the aircraft flow field on the RPV was in the pitch plane.

TABLE OF CONTENTS

LIST OF FIGURES

LIST OF TABLES

NOTATION AND DEFINITIONS

$A_o(z)$	Amplitude variation with separation distance for the mathematical representation of flow field effects; nondimensional
ATA	Aircraft (A-7) angle of attack in the xA-zA plane using the yaw-pitch rotation scheme; positive for nose upward rotation about the yA-axis, degrees
Aircraft (Suffix A)	Parent body (A-7) which causes the flow field through which the RPV travels
Aircraft body axes (xA, yA, zA)	Coordinate axes fixed to the body with triad origin at the aircraft center of gravity (ACG) and parallel to the strain-gage balance axes of the aircraft model; positive forward, starboard, and downward
B	Model span reference dimension, centimeters
Balance axes	Coordinate axes fixed to the store or aircraft model strain-gage balance as appropriate; positive axial, side, and normal forces are rearward, starboard, and upward, respectively
C	Model chord reference dimension, centimeters
C_A	Coefficient of store axial force parallel to the body x-axis, AXIAL/(Q*S); positive in the negative x-direction, nondimensional
C_L	Coefficient of lift force perpendicular to the wind vector, C_N*cos α - C_A*sin α; positive upward, nondimensional
C_{L_α}	Rate of change of C_L with respect to α, per radian
C_{L_o}	Value of C_L for of zero, nondimensional
C_ℓ	Coefficient of store rolling moment about the body x-axis, ROLL/(Q*S*B); positive clockwise, looking in the positive x-direction, nondimensional
$C_{M_{ff}}$	Mathematical representation of RPV pitching moment coefficient variation associated with the A-7 flow field, nondimensional
C_m	Coefficient of store pitching moment about the body y-axis, PITCH/(Q*S*C); positive clockwise, looking in the positive y-direction, nondimensional

C_N	Coefficient of store normal force parallel to the body z-axis, NORMAL/(Q*S); positive in the negative z-direction, nondimensional
$C_{N_{ff}}$	Mathematical representation of RPV normal force coefficient variation associated with the A-7 flow field, nondimensional
C_n	Coefficient of store yawing moment about the body z-axis, YAW/(Q*S*B); positive clockwise, looking in the positive z-direction, nondimensional
C_Y	Coefficient of store side force parallel to the body y-axis, SIDE/(Q*S); positive in the positive y-direction, nondimensional
Captive Trajectory Support (CTS)	Servocontrolled, six-degree-of-freedom wind tunnel auxiliary support used to captively position the RPV model
Downward/Upward	Down/up through the model floor/ceiling irrespective of model position in the tunnel
Mach Number	Mach number of the air in the tunnel test section, air velocity/speed of sound; positive, nondimensional
Port/Starboard	Left/right side as viewed from and rotating with the RPV or aircraft cockpit as appropriate
Q	Dynamic pressure, newtons per square meter
RPV	Remotely piloted vehicle whose static aerodynamics in the flow field of the aircraft are to be determined by a six-component, strain-gage balance
RPV Body Axes (x, y, z)	Coordinate axes fixed to the body with triad origin at the RPV center of gravity (CG) and parallel to the strain-gage balance axes of the RPV model; positive forward, starboard, and downward
S	Model reference area, square meters
V	RPV velocity, positive forward, meters per second
X_{dd}	RPV longitudinal separation distance; positive forward from stored (carry) position, meters

XT-IN, YT-IN, ZT-IN	RPV CG longitudinal, lateral, and vertical positions in the wind tunnel axes. XT-IN referenced 2.54 centimeters model scale downstream of the potential stored (carry) position of the middle pylon on the port wing; YT-IN referenced to the vertical plane containing the aircraft centerline; ZT-IN referenced to the potential carry (stored) position of the middle pylon on the port wing; positive upstream, starboard, and downward, model scale centimeters
z_{dd}	RPV vertical separation distance; positive downward from stored (carry) position, meters
β, α, ϕ	Store angle of sideslip, attack, and roll using the yaw-pitch rotation scheme; β and α referenced to the wind vector and ϕ referenced to the wing level position; positive for nose rotation port about the z-axis, upward about the yawed y-axis, and clockwise looking upstream about the yawed then pitched x-axis, degrees
βT, αT, ϕT	Store angle of yaw, pitch, and roll caused by the mechanical motion of the CTS in the tunnel yaw-pitch rotation scheme; positive for nose rotation port about the ZT-IN axis, upward about the yawed YT-IN axis, and clockwise looking upstream about the yawed then pitched XT-IN axis, degrees
γ	RPV flight path angle; positive upward from the inertial horizontal, degrees
δ_e	Control deflection angle for RPV; positive downward, degrees
θ	RPV pitch attitude; positive nose up from the inertial horizontal, degrees
λ	Flow field wave length for mathematical representation of flow field effects, meters

Angles and directions in the illustration are positive.

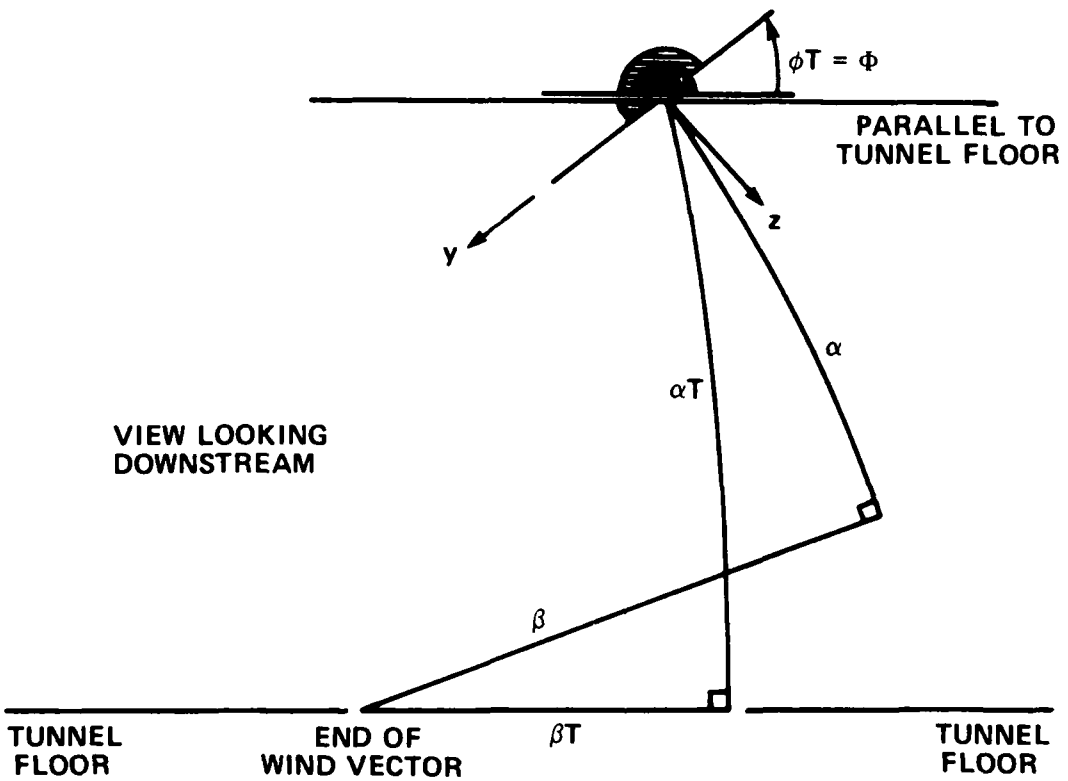

ABSTRACT

A combined wind tunnel/computer analysis was undertaken to evaluate the aerodynamic feasibility for airborne recovery of a fixed-wing remotely piloted vehicle (RPV). A map of aerodynamic loads interacting on the aircraft and RPV was obtained in the wind tunnel. The flow field was then represented mathematically and used to evaluate the aerodynamic feasibility of airborne retrieval. It was concluded that retrieval forward of the aircraft is potentially dangerous, unless a separation of more than two meters is maintained; retrieval aft of the aircraft is aerodynamically safe without restriction. In addition, it was determined that the primary effect of the aircraft flow field on the RPV was in the pitch plane.

ADMINISTRATIVE INFORMATION

This feasibility investigation was undertaken by the Aircraft Division (1660) of the Aviation and Surface Effects Department (16) of the David W. Taylor Naval Ship Research and Development Center (DTNSRDC). The program was sponsored by the Remotely Piloted Vehicle Project Office (PMA 247) of the Naval Air Systems Command (NAVAIR) and was funded under Task Area W3359, Work Unit 1660-253.

INTRODUCTION

BACKGROUND

The U.S. Navy has a long history of involvement with remotely piloted vehicles (RPV's) but only at a relatively low level. Significant advances in lightweight avionics and sensor technologies along with growing concern over the use of piloted aircraft in politically sensitive areas led to major RPV developments for Southeast Asia.

Recovery of an RPV following completion of a mission is obviously an important economic consideration. In fact, recovery is the driving factor in the successful deployment of these vehicles, and considerable effort has been devoted to evolving retrieval techniques aboard ship. Recovery of RPV's by airborne platforms could increase the RPV range and mission objectives, and these potential advantages warrant investigation.

OBJECTIVE

The present study was undertaken to determine the feasibility of airborne retrieval of an RPV. Models of a fixed-wing RPV and the A-7 CORSAIR II were chosen, and the aerodynamic effects caused by their interaction were investigated in a wind tunnel at low speeds. A mathematical representation of the flow fields of these crafts was undertaken to determine major problem areas in airborne retrieval.

DESCRIPTION OF THE MODELS

The aircraft model was a 0.10 scale LTV A-7 CORSAIR II configured with a flow-through inlet and six parent pylons. A 0.10 scale model of a MK-83 low-drag bomb was mounted on the middle pylon of the starboard wing to simulate weight and aerodynamic counterbalance. A level flight cruise condition at altitude was simulated by setting the A-7 model to +5.0-degree fuselage reference plane angle of attack (ATA) and the horizontal stabilizers to a -10.0-degree angle of incidence.

The RPV was also a 0.10 scale model with fixed wing and tail. The engine inlet was faired over with a smooth fairing since the scale did not permit a flow-through model.

Transition was fixed on the fuselage, wing, and tail of the A-7 model and on the fuselage and wing of the RPV model by using the simplified method of Braslow and Knox[1].

PROCEDURE

All investigations were performed in the DTNSRDC 7- by 10-foot wind tunnel at a Mach number of 0.385, a dynamic pressure (Q) of 9576 N/m^2 and a Reynolds number of $7.62 \times 10^5/m$. The captive trajectory support (CTS) was used in conjunction with the main support to position both models on six-component strain gage balances. The resulting map of aerodynamic loads in the interactive flow field was used to evaluate the aerodynamic feasibility of airborne retrieval in the zone of coverage. This flow field was mathematically generalized and combined with such RPV characteristics as control power, moments of inertia, and weight to perform studies in a computerized set of motion equations.

DUAL STING INSTALLATION

In the captive model technique, a geometrically scaled model is mounted on a sting support by means of an internal strain-gage balance. The sting support is a remotely controlled mechanical system used to

---

[1]Braslow, A.L. and Knox, E.C., "Simplified Method for Determination of Critical Height of Distributed Roughness Particles for Boundary-Layer Transition at Mach Numbers from 0 to 5," National Advisory Committee for Aeronautics Technical Note 4363, September 1958.

provide various attitudes and positions of the model relative to the wind orientation. The internal strain-gage balance is an electromechanical unit that indicates the static aerodynamic load for a given attitude and position of the model. For this particular experiment, a separate sting support/balance was used in both the RPV and aircraft models.

The aircraft model was mounted on the main support which has two degrees of freedom. Although the support is capable of being remotely changed in either two attitudes (yaw, pitch) or one attitude (pitch) and one position (lateral), the aircraft model was positioned only in pitch. The RPV model was mounted on the CTS which has six degrees of freedom. The test plan required the use of the complete system capabilities for remotely controlling three attitudes (yaw, pitch, and roll) and three positions (longitudinal, lateral, and vertical). Figure 1 shows the typical installation of a model/support system with dual-sting arrangement. The ranges of travel for the CTS are given in Figure 2. To permit close-in positioning of the RPV with respect to the aircraft, a 15.24 cm offset sting was used as shown in Figure 3.

EXPERIMENTAL TECHNIQUES

Three distinct captive model techniques were used in the experiment to acquire the required spectrum of information: (1) an isolated data phase to obtain free-stream isolated data, (2) a modified grid phase to map the aerodynamic loads experienced by the RPV over a finite range of attitudes and positions while in the interference flow field of the A-7, and (3) a retrieval path phase to record aerodynamic loads experienced by the RPV at zero attitude while on planned travel excursions from the interference flow field of the A-7 to the CTS position limits.

Isolated Data Phase

After completion of the tunnel installation and checkout, it was necessary to isolate the models from their interactive flow fields in order to acquire free-stream aerodynamic data for the RPV. To achieve this, the RPV model was positioned as far as possible beneath and forward of the A-7 model. Two runs were necessary for both the normal and lateral plane information. Run 7 was a pitch sweep of ±30 degrees while yaw and roll were equal to zero. Run 8 was a yaw sweep of ±30 degrees while pitch and roll were equal to zero.

Modified Grid Phase

This scheme permitted the semiautomatic acquisition of large amounts of accurate RPV data while covering a predetermined grid in proximity to the retrieval aircraft. The A-7 model was set to the conditions listed previously. The combination of yaw (βT), pitch (αT), roll (ϕT) and lateral (YT-IN) position for the RPV center of gravity (CG) was manually controlled by potentiometer settings. The CG was then positioned to a known reference point (XT-IN, ZT-IN) with respect to the A-7. From this known reference, the CTS was then engaged in the automatic mode and data were taken while the RPV vertical (ZT-IN) position was moved toward the A-7 model until contact was made with the A-7 or the main support. The motion was then reversed to a predetermined distance from the A-7 model; an increment forward longitudinally (XT-IN) was then made and the vertical (ZT-IN) sweep was repeated. Five longitudinal (XT-IN) stations were used for the vertical (ZT-IN) in and out data by taking sweeps of a given automatic run. Figure 4 is a scaled bottom

view showing the CG locations (XT-IN = -33.0, -16.5, 0.0, 16.5, 33.0 cm, model scale) relative to the A-7 for a given run.

The scaled sketch shown in Figure 5 is a front view for the three lateral locations (YT-IN = -19.61, -24.69, -34.70 cm, model scale) chosen to be covered for all runs along with the minimum vertical depth (ZT-IN = 43.2 cm, model scale) covered for any given run. In all, 34 runs were used to cover the grid beneath the A-7 model. The nominal conditions for these runs are listed in Table 1.

Retrieval Run Phase

The data from this scheme served two basic purposes: (1) they partially expanded the position coverage of the modified grid phase, and (2) they enabled a quick check for possible rapid aerodynamic gradients in the A-7 flow field. The A-7 model was set to the conditions listed previously. All runs were made with yaw, pitch, and roll set to zero. The intent was to take data while making vectored excursions of the RPV model from within the A-7 flow field out to the CTS position limits of travel. The combination of one to three positions was simultaneously varied to give a special straight line retrieval path for each run. The area covered with this rough position grid was much larger than with the modified grid. The resulting position and balance data can be used to quickly determine major problem areas of retrieval. The conditions and maximum limits of coverage for the six runs are listed in Table 2.

TABLE 1 - MODIFIED GRID RUNS

(Nominal run schedule for the 0.10 scale RPV at Mach 0.385 beneath the 0.10 scale A-7 at an ATA of 5.0 degrees (-3.0 degrees rack incidence) and sideslip of 0.0 degree)

Run* Number	α degree	β degree	ϕ degree	YT-IN (Lateral)
21	-5.00	0	0	-34.70
18	0			
27	5.00			
31	10.00			
34	15.00			
50	-5.00	0	-30.00	-24.69
47	0			
42	5.00			
38	10.00			
67	15.00			
20	-5.00	0	0	
17	0			
68	2.0			
53	2.3			
26	5.00			
30	10.00			
33	15.00			
52	-5.00	-15.00	0	
46	0			
43	5.00			
37	10.00			
51	-5.00	15.00	0	
45	0			
44	5.00			
36	10.00	15.00	0	-24.69
49	-5.00	0	30.00	
48	0			
41	5.00			
39	10.00			
22	-5.00	0	0	-19.61
19	0			
29	5.00			
32	10.00			
35	15.00			

*A run consisted of approximately 43.2 cm of ZT-IN in and out sweep at the following XT-IN stations: -33.0, -16.5, 0.0, 16.5, and 33.0 cm.

TABLE 2 - RETRIEVAL RUNS

(Nominal run schedule for the 0.10 scale RPV at Mach 0.386 beneath the 0.10 scale A-7 at an ATA of 5.0 degrees (-3.0 degrees rack incidence) and sideslip of 0.0 degree)

Run* Number	α degree	β degree	ϕ degree	XT-IN Maximum Value, cm	YT-IN Maximum Value, cm	ZT-IN Maximum Value, cm
Rearward Retrieval						
54	0	0	0	-79	-64	84
55	0	0	0	-79	Fixed -24.69	84
Sideway Retrieval						
56	0	0	0	- 3	-64	84
64	0	0	0	0	-58	Fixed 31
Forward Retrieval						
62	0	0	0	53	-58	84
63	0	0	0	53	Fixed -24.69	84

*A run consisted of a vectored excursion from a reference position within the flow field to the listed limits and a return to the same reference position.

DATA REDUCTION

The balance signals, attitude, position, and tunnel information were recorded on magnetic tape from a Beckman 210 high-speed data acquisition system. The balance data were processed through amplifiers with 5-Hz filters. The resulting raw data tape was used as input to a XDS 930 digital computer along with reference information, data reduction sensitivities, balance integration constants, and data reduction equations. The attitudes (βT, αT, ϕT, ATA) and positions (XT-IN, YT-IN, ZT-IN) were corrected for the aerodynamic load deflections of both models by using previously determined load/deflection sensitivities. The resulting attitudes and positions were accurate to within the values presented in Table 3. The RPV model balance data represent the averages of three readings recorded 20 msec apart. The aircraft model balance data consist of a single recording per data point. The balance data were reduced to the form of body-axes nondimensional coefficients by the formulas

$$C_{FORCE} = \frac{FORCE}{Q*S} \text{ and } C_{MOMENT} = \frac{MOMENT}{Q*S*B(C)}$$

This gave three force (axial, side, normal) coefficients and three moment (roll, pitch, yaw) coefficients for each model. The moment coefficients were then transferred to the desired full-scale moment reference station. Table 4 lists the reference dimensions used for all data reductions. Repeatability readouts and accuracy checks indicated that resolutions of the balance coefficient systems were as listed in Table 5. The data were not corrected for tunnel blockage or base pressure, but these are felt to have little overall effect on this specific investigation.

TABLE 3 - ATTITUDE AND POSITION ACCURACIES

Item	Value
βT	0.10 degree
αT	0.10 degree
ϕT	0.25 degree
XT-IN	0.051 cm
YT-IN	0.051 cm
ZT-IN	0.064 cm
ATA	0.05 degree

TABLE 4 - REFERENCE INFORMATION

Item	RPV	A-7
Scale	0.10	0.10
S (Wing Area), m^2	0.0074	0.3484
B (Wing Span), cm	17.63	118.049
C (Wing Chord), cm	4.399	33.056
Moment Reference Station, cm		
Longitudinal (nose to 1/4 chord)	19.74	70.33
Vertical (downward)	0.20	0.0

TABLE 5 - COEFFICIENT RESOLUTION

Coefficient	RPV	A-7
C_A	0.003	0.001
C_Y	0.013	0.008
C_N	0.016	0.012
C_L	0.016	0.012
C_ℓ	0.002	0.002
C_m	0.006	0.003
C_n	0.002	0.002

ESTABLISHMENT OF CONFIDENCE FACTOR

Data taken during the isolated run phase were compared to data from a prior larger scale, low-speed investigation at Cal Tech in order to establish a confidence factor for overall data levels. Planned differences in the models must be noted to put the comparison into proper perspective. The 0.40 scale RPV model had tanks/pods on both wing tips whereas the 0.10 scale model of the present study had no tanks/pods. Moreover the larger scale model had a -1.0 degree horizontal stabilizer incidence compared to an intentionally decreased incidence of -2.0 degrees for the smaller model.

In view of these intentional differences between models, the agreement for lift coefficient (C_L) versus angle of attack (α) was good; see Figure 6. The slightly different C_{L_α} (4.18/rad versus 5.02/rad) over the -5.0- to +10.0-degree α range is attributed to the lack of endplate effect caused by the wing tip arrangement. The shift in C_{L_o} (0.014 versus 0.034) is probably due to the horizontal stabilizer incidence. The earlier stall is indicative of the smaller scale effect.

A plot (Figure 7) of pitching moment (C_m) versus angle of attack (α) indicates that all the data fell within a general coefficient band. However, the smaller scale moment showed a general trend to increased stability.

Figure 8 is a plot of lateral plane information for a range of ±20.0-degree angle of sideslip (β). Agreement for side force coefficient (C_Y) was very good. There was some discrepancy for rolling moment (C_ℓ), but the generally expected nonlinearity was evident in both sets of data. Data on yawing moment (C_n) disagreed somewhat, but that for the

smaller model had a better intercept for a mirror symmetry configuration. It should be noted that agreement for C_ℓ and C_n would have been better had the larger scale data shifted to the zero intercept as theoretically expected. The coefficient resolutions for the smaller scale data of Figures 6-8 are shown and should be noted for C_ℓ and C_n.

Agreement for the axial coefficient levels (0.030 versus 0.035, not presented in plotted form) was considered good in view of the respective sizes of the models.

ANALYSIS AND RESULTS

The spatial gradients on RPV forces and moments due to the presence of the A-7 were analyzed together with the effect of such gradients on motion of the RPV while transversing the flow field in proximity to the aircraft.

VERTICAL POSITION

The effect of vertical (ZT-IN) position on normal force (C_N), pitching moment (C_m), and axial force (C_A) is shown in Figure 9. These data were taken at a constant (XT-IN)-(YT-IN) position corresponding to the stored (carry) pylon location. Gradients exist in the ZT-IN separation region from 0 to 20 cm, but the influence of the A-7 was negligible at separation distances greater than 20 cm (2 m full scale).

Further examination of the data indicated stable and safe gradients in this area (ZT-IN < 20 cm). As the RPV was moved closer to the A-7, there was a loss in normal force, a nose-down pitching moment, and a slight increase in axial force. All of the above characteristics indicate

that the RPV must be actively flown to the A-7 and that the possibility of collision is small if control of the RPV is lost. Moreover, there was little change in C_{N_α} or C_{m_α} with aircraft proximity, thus negating the necessity of any changes in the basic automatic pilot system of the RPV. The effect of lateral (YT-IN) location on normal force, pitching moment, and rolling moment is shown in Figure 10. No trends were noted in side force or yawing moment, and therefore, these data are not presented.

LONGITUDINAL POSITION

The effect of longitudinal (XT-IN) location on C_m and C_N is indicated in Figure 11 for four longitudinal stations: -16.5 cm aft of the stored (carry) position, at the stored (carry) position, and at two forward stations corresponding to 16.5 cm and 33.0 cm. A strong nonlinear gradient occurred in both pitching moment and normal force. The gradient in pitching moment took the form of a nose-up pitching moment followed by a rapid nose-down moment which remained constant to a distance 16.5 cm aft of the stored (carry) position. Similarly, normal force increased and then decreased as XT-IN decreased. The pitching moment gradient is a major concern. The range of pitching moment coefficient exhibited (+0.05 to -0.05) is equivalent to a 10-degree elevator doublet input. It can also be seen that the magnitude of this pitching moment coefficient increased with vertical proximity of the aircraft.

CLOSURE ANALYSIS

A three-degree-of-freedom, closed-loop trajectory program was utilized to evaluate the response of the RPV to the above longitudinal

and vertical gradients. Representative full-scale inertia, damping derivatives, and control terms were utilized as inputs to the closed-loop trajectory program. The control system was represented by a closed-loop, attitude-hold system utilizing both proportional and rate feedback. Gains for these feedbacks were, respectively, 0.01 deg/deg and 0.005 deg/deg/sec.

The flow field used was

$$C_{M_{ff}} = A_o(z) \sin\left(\frac{2\pi}{\lambda} * x_{dd}\right)$$

$$C_{N_{ff}} = -A_o(z) \cos\left(\frac{2\pi}{\lambda} * x_{dd}\right)$$

where λ is the flow field wave length.

The variation of amplitude with vertical distance, $A_o(z)$, is shown graphically:

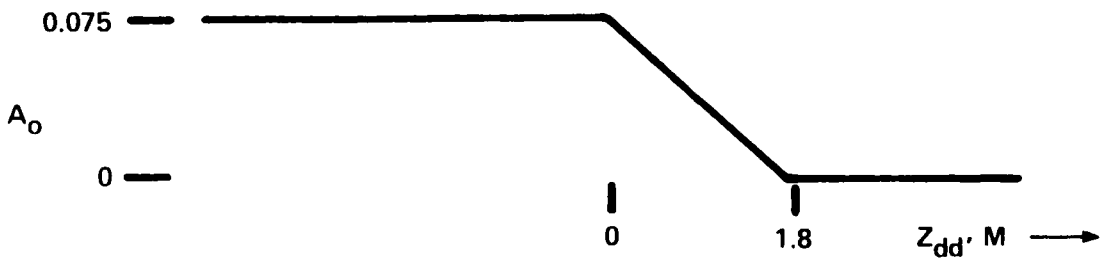

As previously discussed, it was assumed that there were no flow field effects at separations greater than 2 m full scale.

Approaches into the flow field were made in two ways: (1) a forward closure wherein the aircraft (i.e., flow field) overtakes the RPV and

(2) an aft closure wherein the RPV overtakes the aircraft. These are shown below:

FORWARD CLOSURE (VA > V)

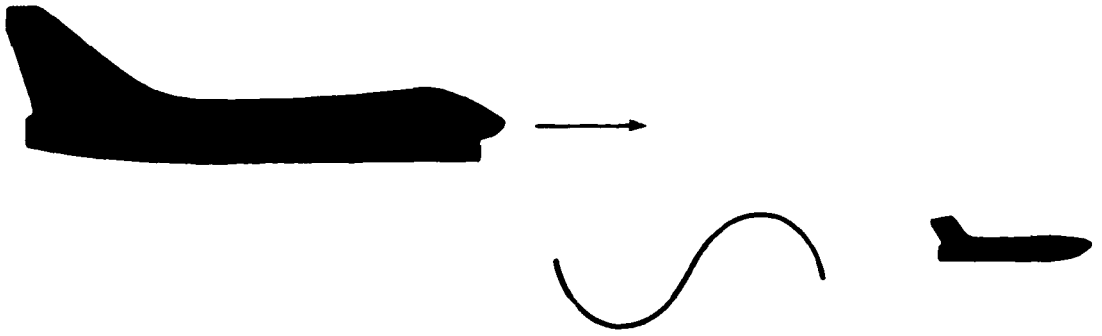

AFT CLOSURE (VA < V)

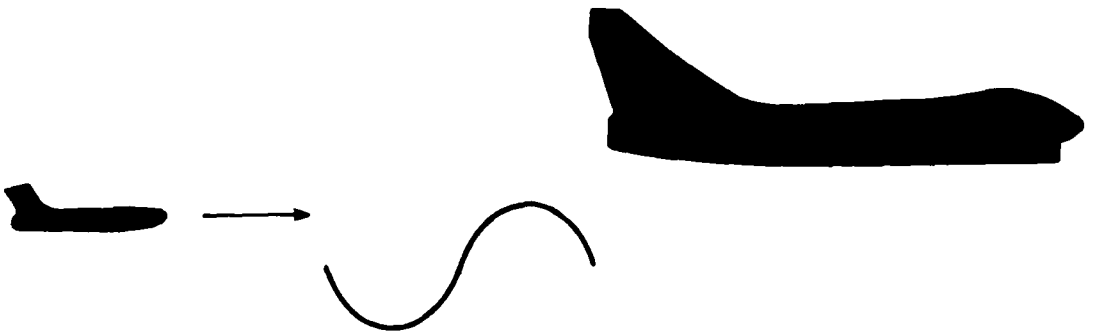

In both cases the RPV was assumed to be initially trimmed at a velocity of 122 m/s and an altitude of 3048 m. The effect of such variables as closure speed, flow field wave length, and the open-loop characteristics of the system are presented in the following sections.

Figure 12 indicates the open-loop characteristics of the vehicle for the two closure cases at a wave length of 3 m. For the aft closure case (i.e., RPV overtakes aircraft), the RPV entered the flow field, was given a nose-down moment, and left the vicinity of the aircraft. In this case, the pitch oscillation was rapidly damped. For the forward

closure case, on feeling the influence of the flow field, the RPV experienced a large nose-up pitch and began a climb into the path of the aircraft. This is obviously an unsafe situation and would likely result in collision if control of the RPV were lost.

The effect of flow field wave length on forward and aft closures is shown in Figures 13 and 14, respectively. These configurations were flown closed loop with a closure speed of 0.6 m/s and initial Z_{dd} separations of 1.2 m and 0.6 m, respectively. For forward closure (Figure 13), the long wave length flow field caused a large Z_{dd} excursion of 4 m and then a rapid decrease in altitude. The shorter wave length significantly decreased the Z_{dd} excursion to approximately one-half the value, i.e., 2 m. For both wave lengths, the control system minimized the pitch excursion.

The decrease in altitude excursion is attributed principally to the fact that the flow field has approximately the shape of a doublet control input; if the input is sharp enough (i.e., short time), only the short period mode will be affected and no altitude excursion will occur.

For the aft closure case (Figure 14) the RPV lost approximately 1.5 m of altitude for both wave lengths with little excursion in pitch or angle of attack.

The effect of closure rate is shown in Figure 15 for the forward closure case at closure speeds of 0.6 and 1.5 m/s. As indicated in the figure, altitude excursion was reduced by increasing closure speed. Once again this is a result of the shorter time in which the flow field can act on the RPV. A similar comparison for the aft closure revealed no significant changes for that approach.

The above comparisons between aft and forward closure indicate that aft closure is relatively safe (aerodynamically); whereas, forward closure is potentially dangerous. Underneath the wing near the stored (carry) pylon location, the RPV tends to nose down and away from the aircraft; whereas, forward of the aircraft wing, the RPV tends to nose up into the aircraft.

The above results, however, do not completely negate the possibility of forward closure inasmuch as that procedure is relatively safe provided a separation of greater than 2 m can be maintained between the RPV and the recovery aircraft.

CONCLUSIONS

The following conclusions have been drawn from analysis of the data:

1. An aerodynamically safe retrieval is feasible if the RPV approaches aft of the aircraft. Loss of control of the RPV results in the RPV moving away from the aircraft.

2. If the aircraft is overtaking the RPV, a forward approach, an aerodynamically hazardous situation results if control of the RPV is lost.

3. The influence of the aircraft on the RPV is negligible at vertical full scale separation distances greater than 2 m.

4. Due to the nature of the flow field, the RPV must be actively flown to the aircraft attachment point.

5. The primary interference effects are generated in the pitch or normal plane.

6. Increasing closure speed reduces the RPV's vertical excursion as there is less time for the flow field to act on the RPV.

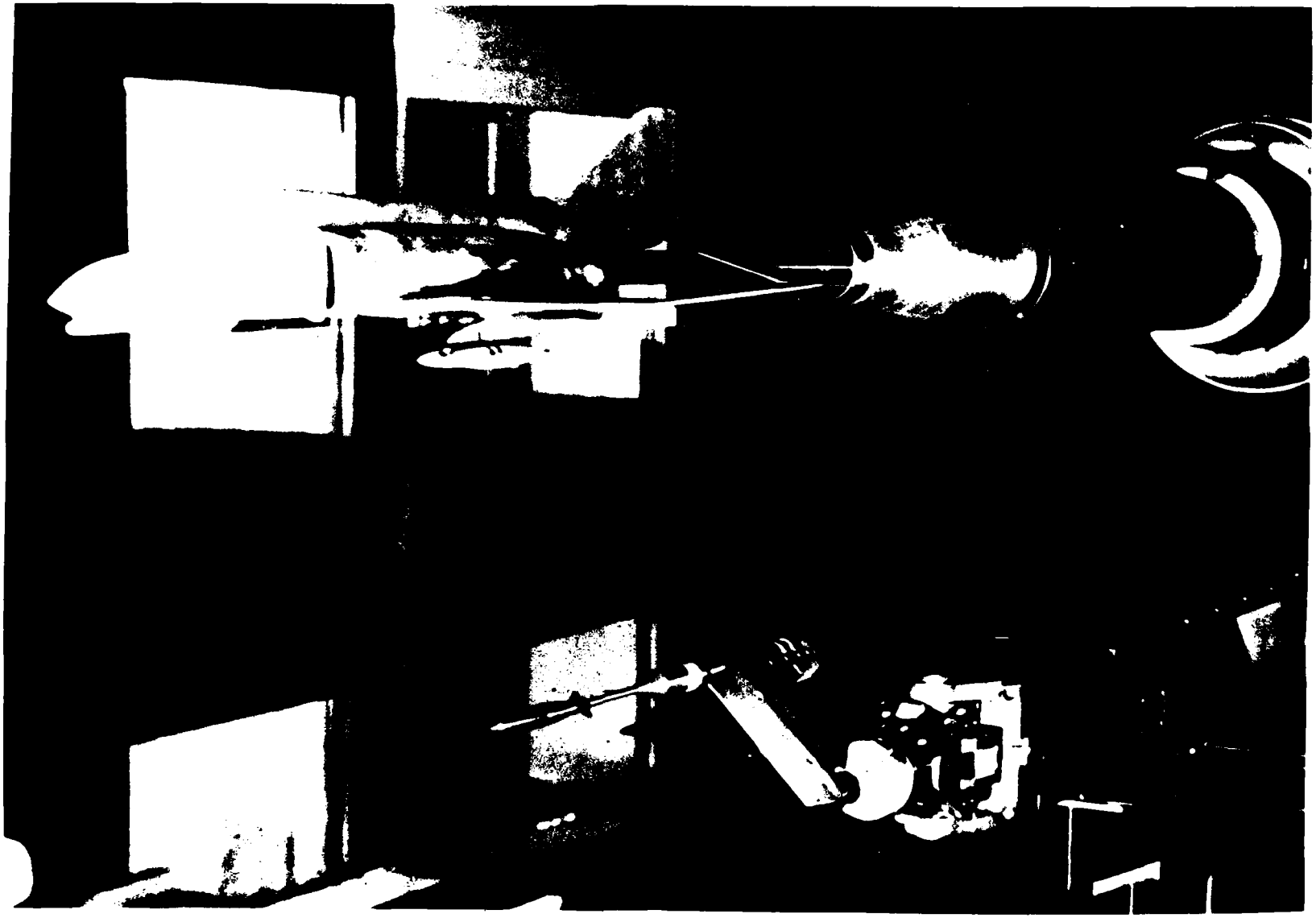

Figure 1 - Typical Installation of CTS-Mounted Store and Main-Support-Mounted Aircraft Model in the DTNSRDC 7- by 10-Foot Transonic Wind Tunnel

Figure 2 - Envelope of Motion for the Captive Trajectory Support

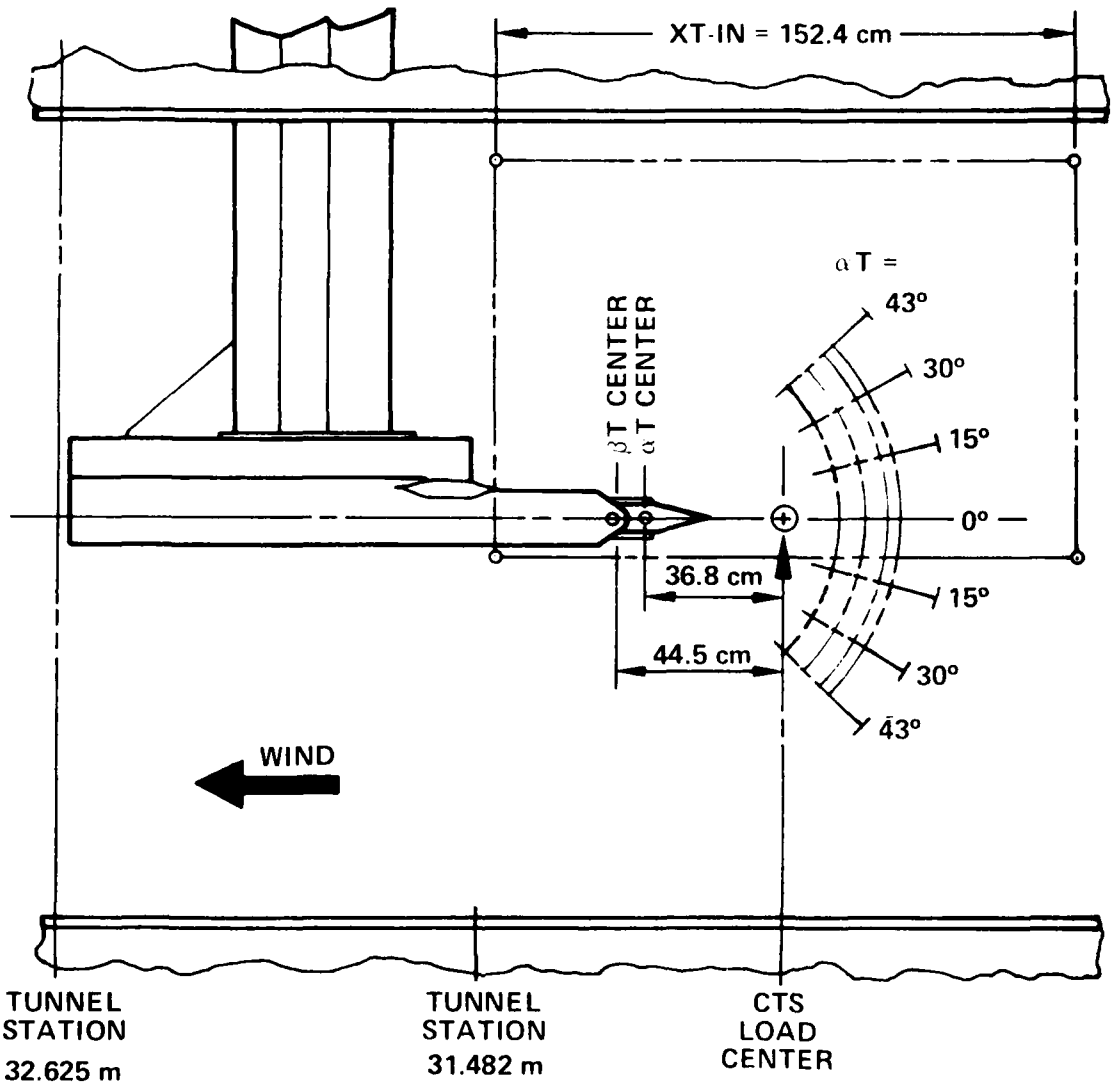

Figure 2a - Side View

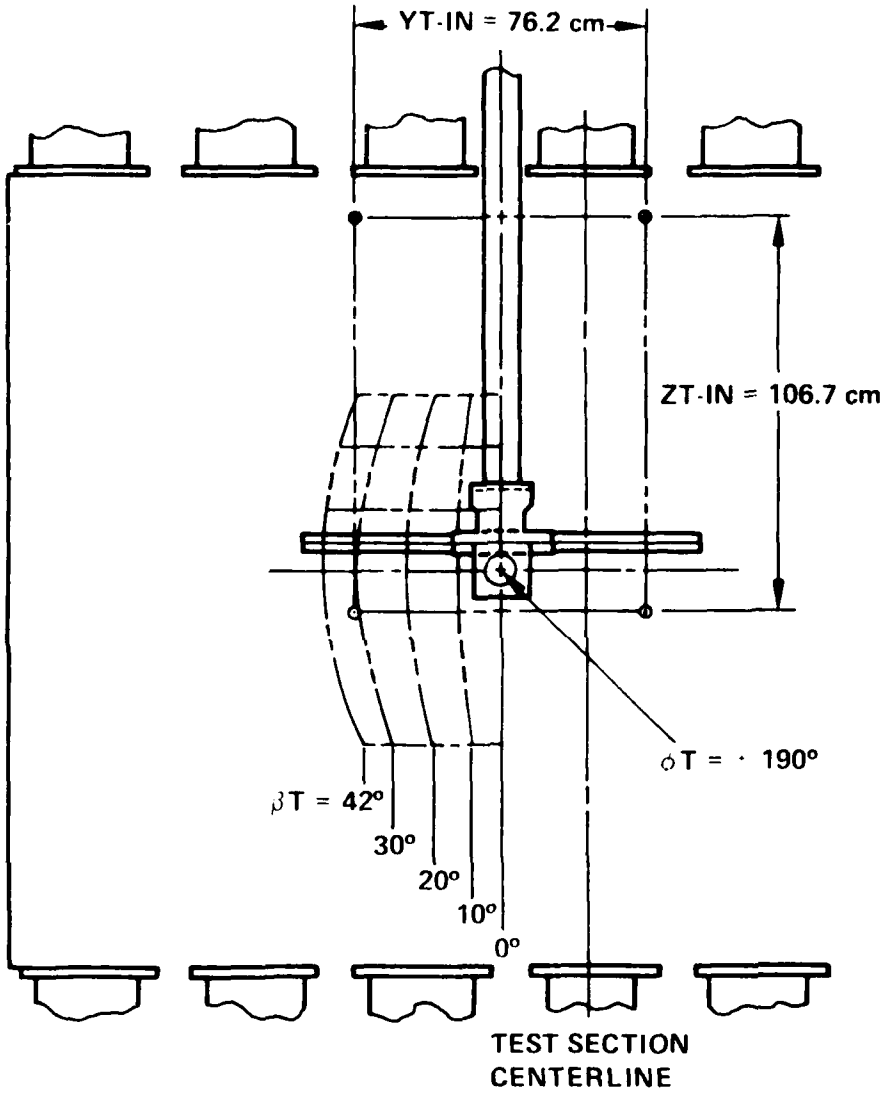

Figure 2b - Front View

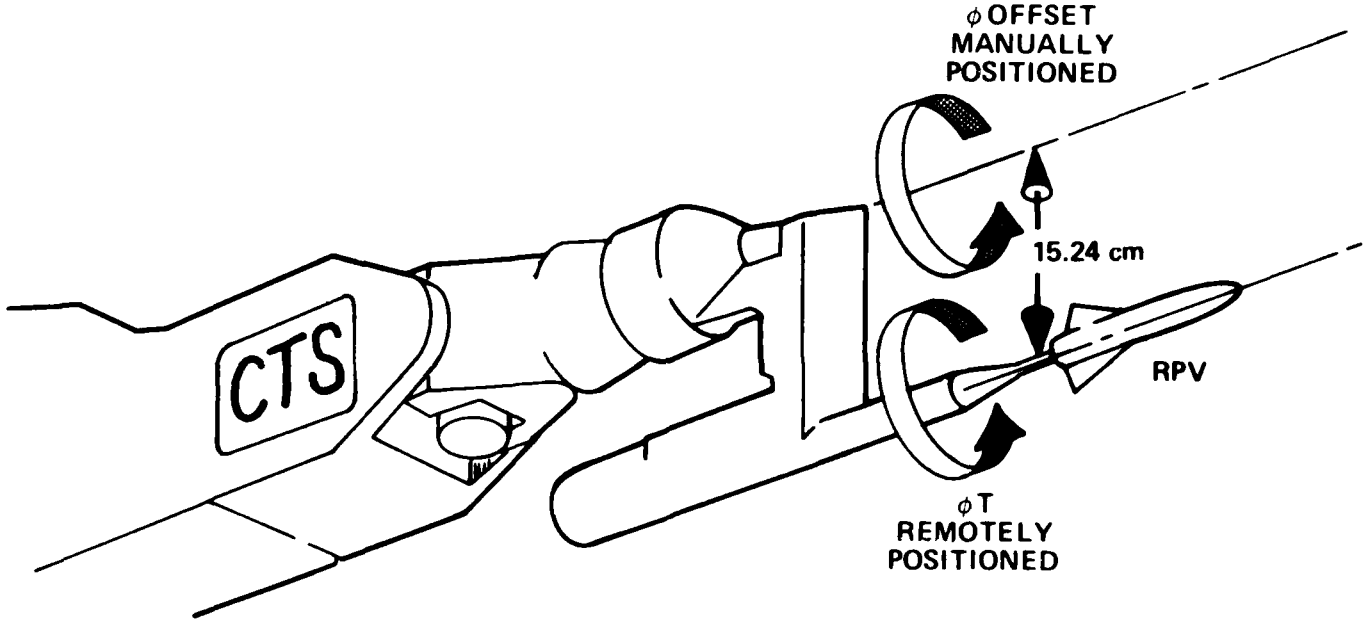

Figure 3 - Details of the 15.24 Centimeter Offset Sting

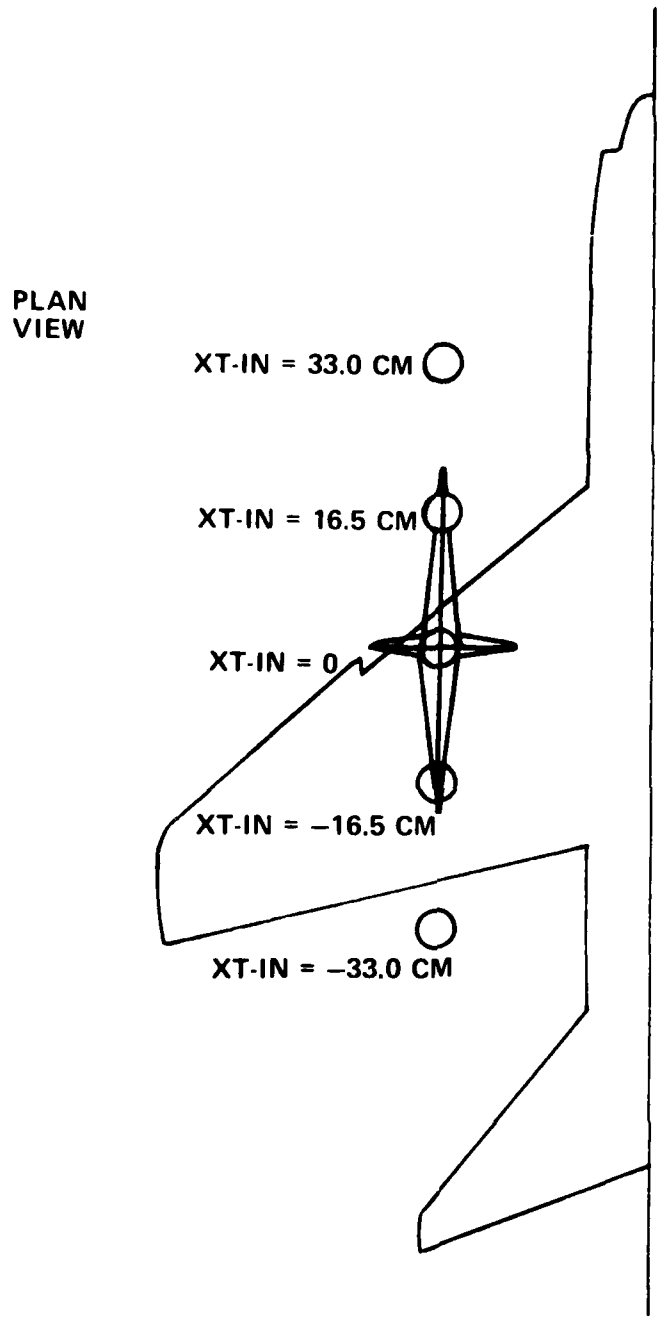

Figure 4 - RPV Longitudinal Location with Respect to the A-7

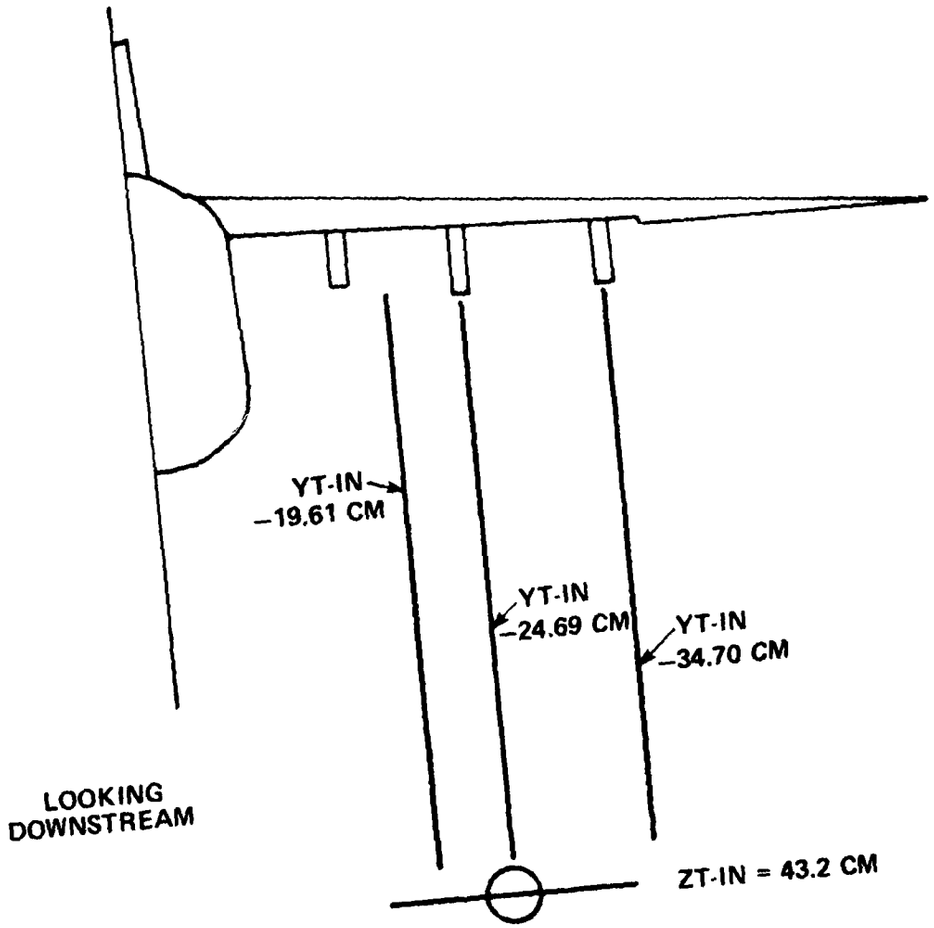

Figure 5 - RPV Lateral and Vertical Locations with Respect to the A-7

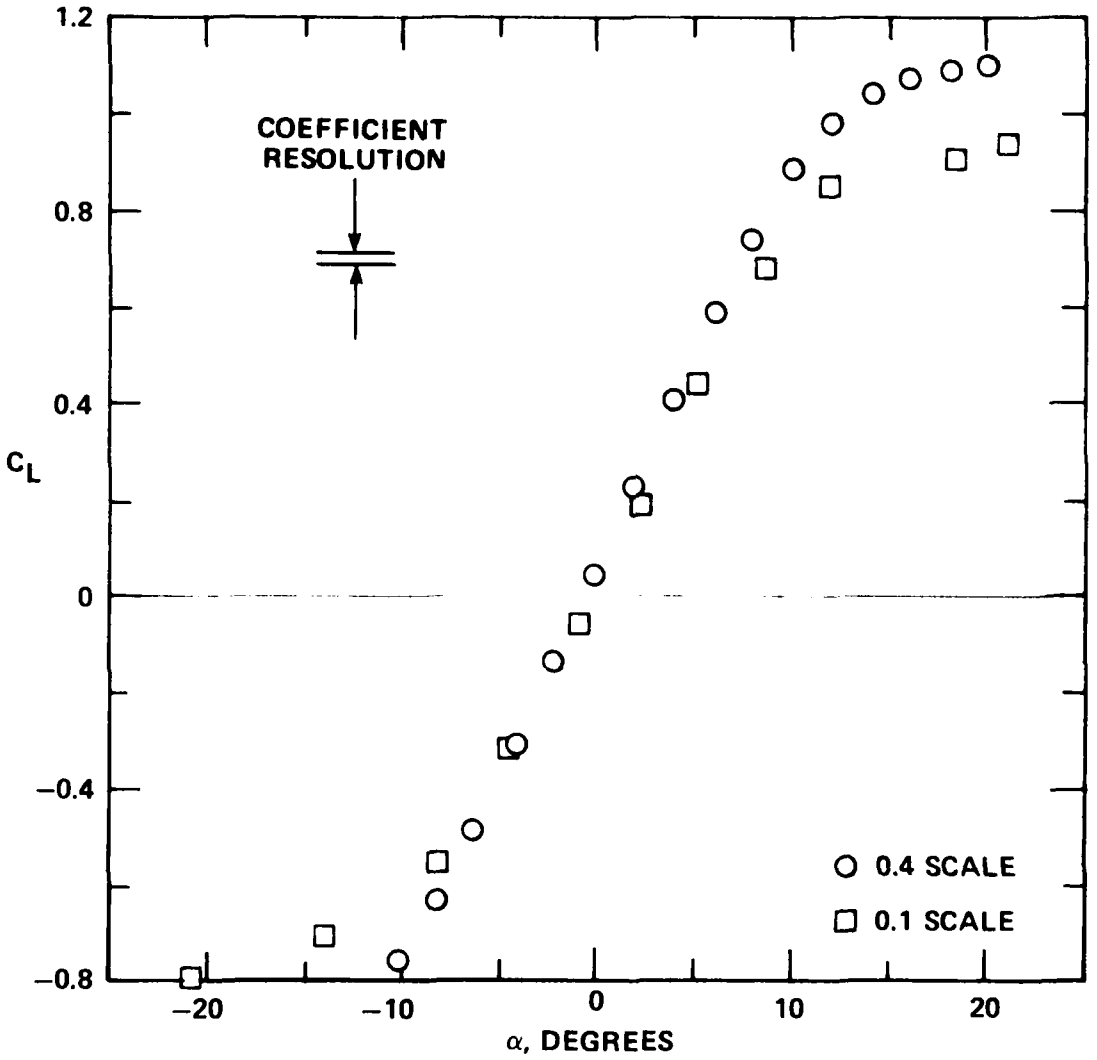

Figure 6 - RPV Isolated Lift Coefficient Versus Angle of Attack

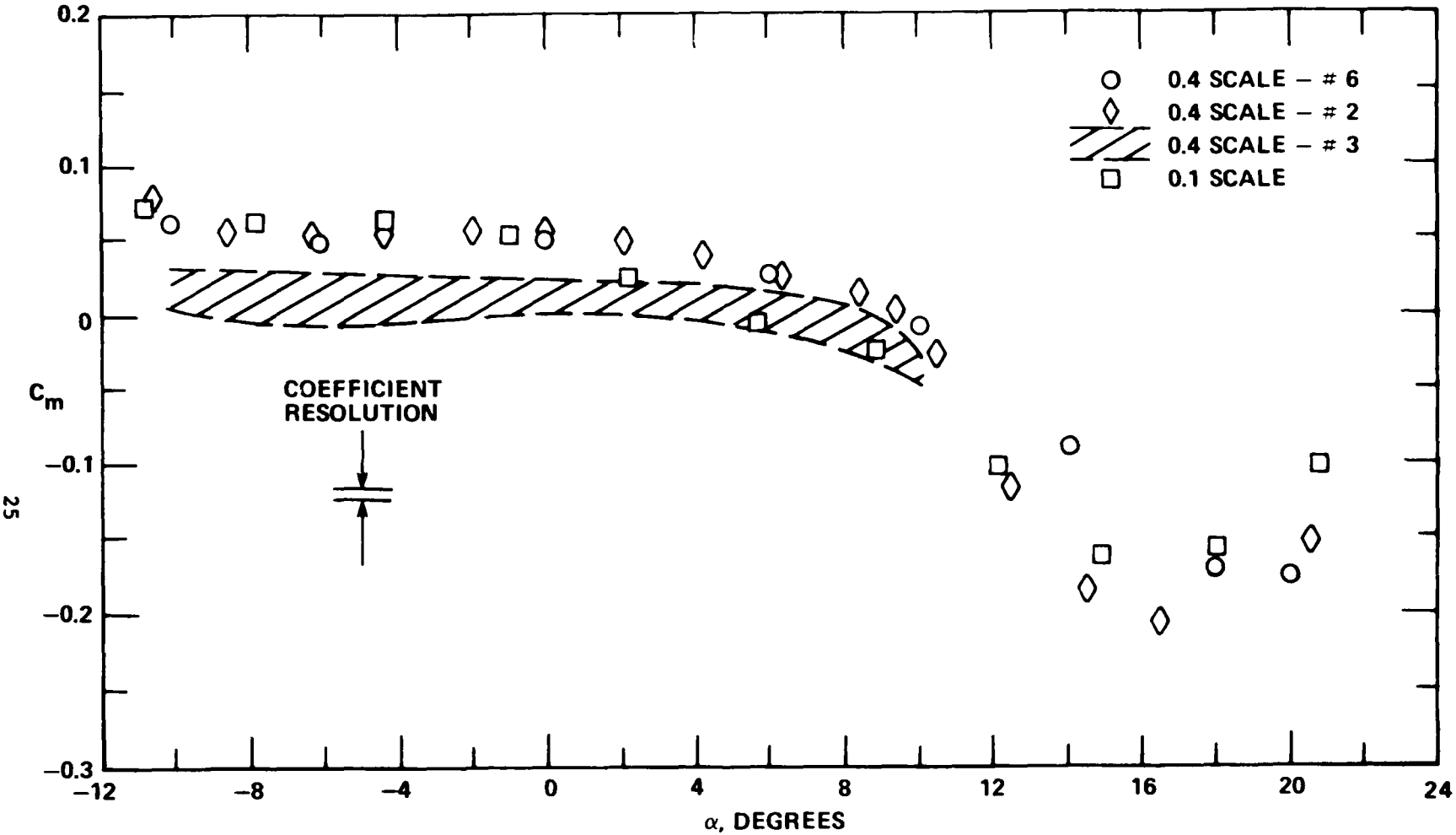

Figure 7 - RPV Isolated Pitching Moment Coefficient Versus Angle of Attack

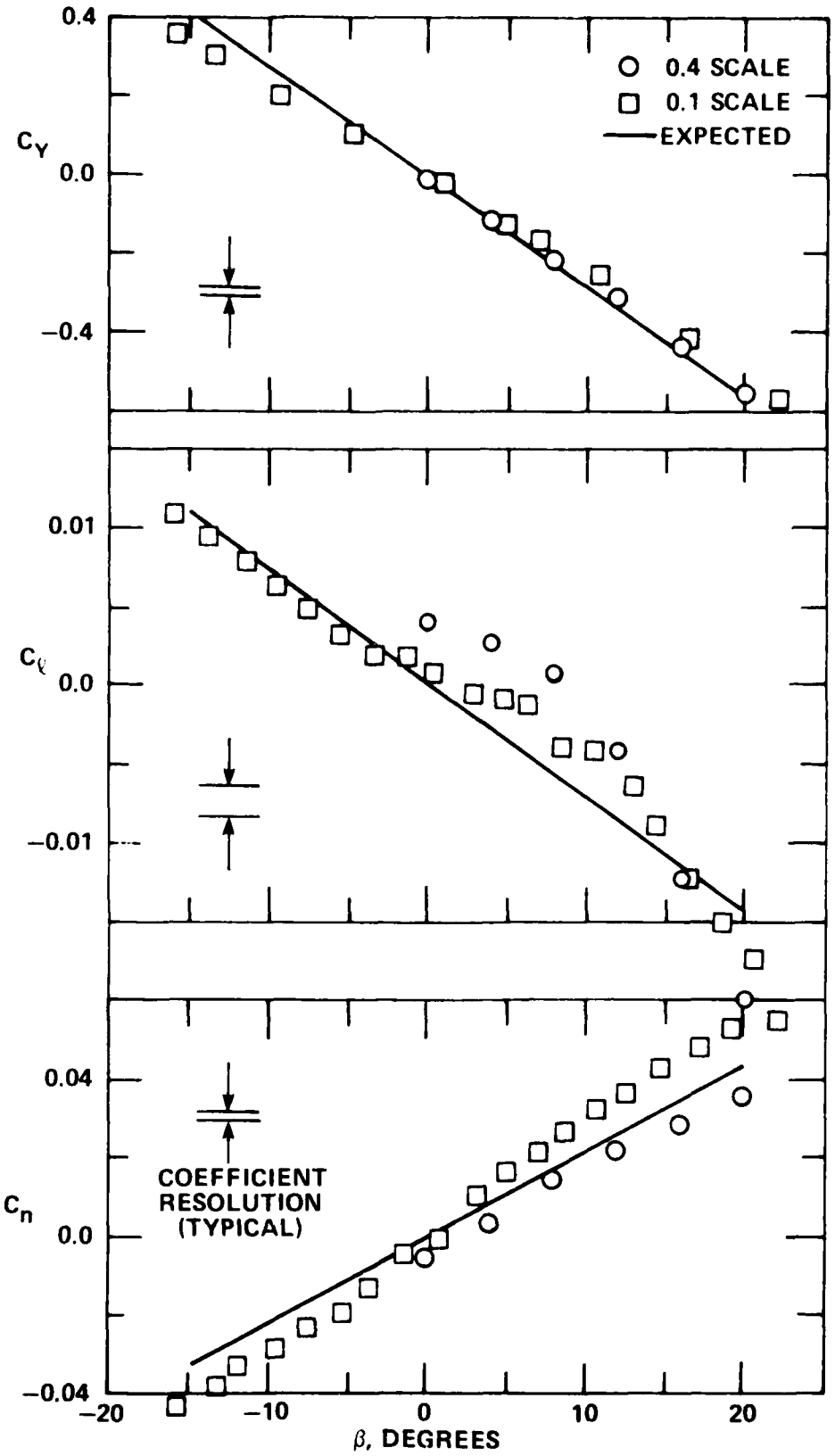

Figure 8 - RPV Isolated Lateral Coefficient Versus Angle of Sideslip

Figure 9 - Effect of Vertical Position at Various Angles of Attack

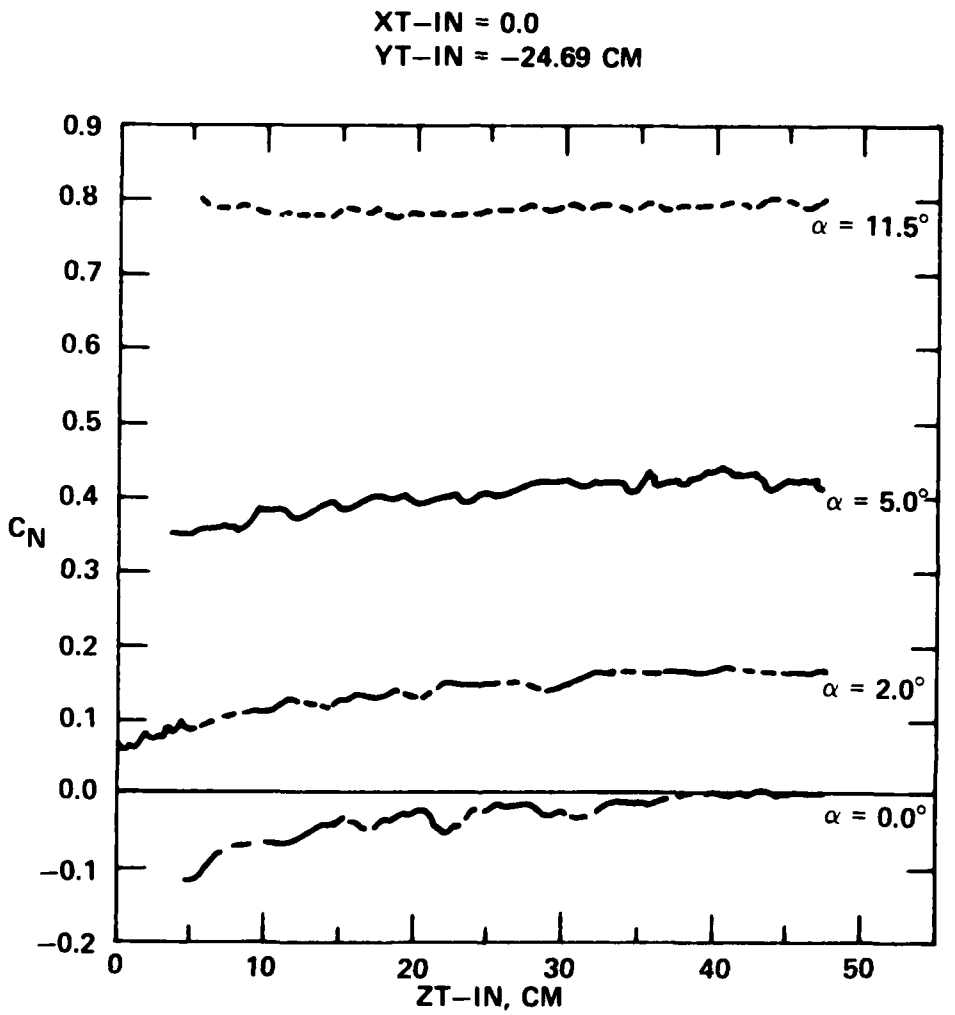

Figure 9a - On Normal Force Coefficient

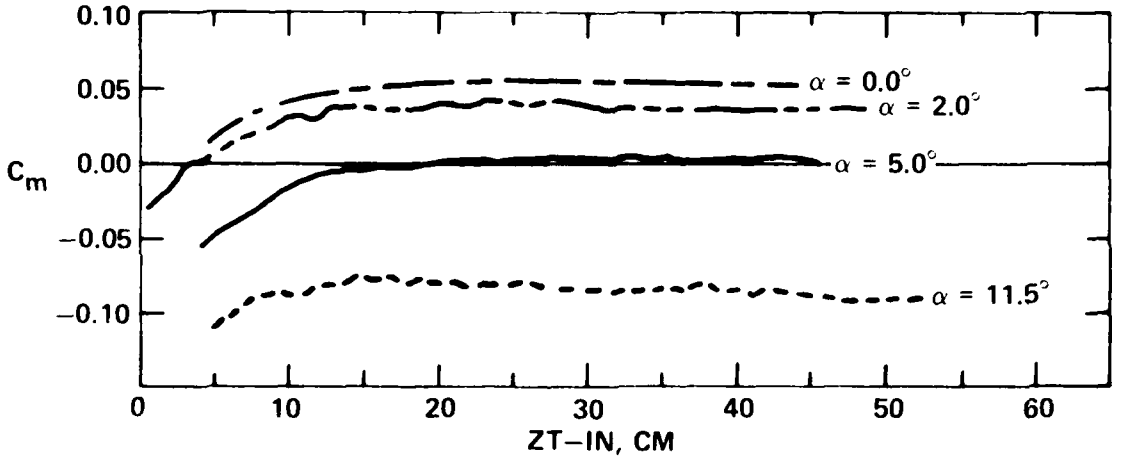

Figure 9b - On Pitching Moment Coefficient

XT−IN = 0.0
YT−IN = −24.69 CM

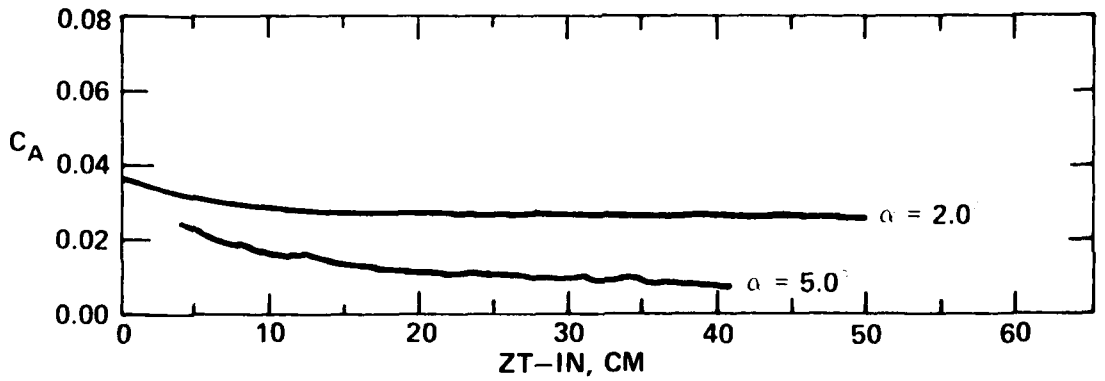

Figure 9c - On Axial Force Coefficient

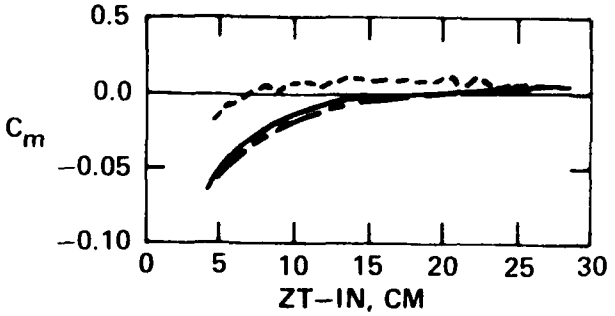

Figure 10a - On Pitching Moment Coefficient

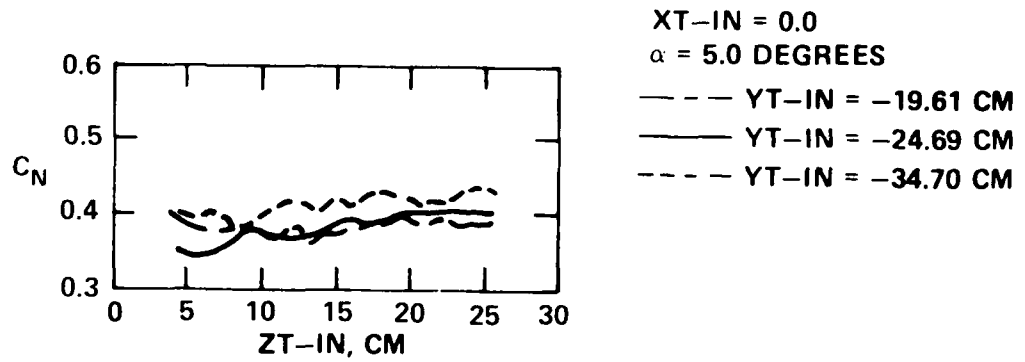

Figure 10b - On Normal Force Coefficient

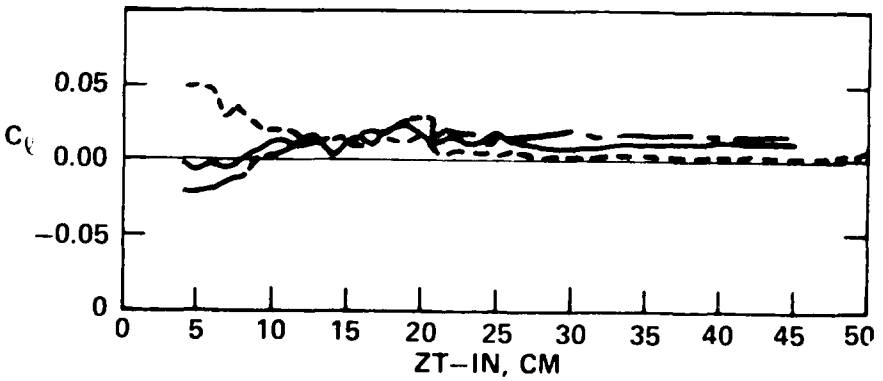

Figure 10c - On Rolling Moment Coefficient

Figure 10 - Effect of Vertical and Lateral Locations on C_m, C_N, and C_ℓ at XT-IN = 0.0

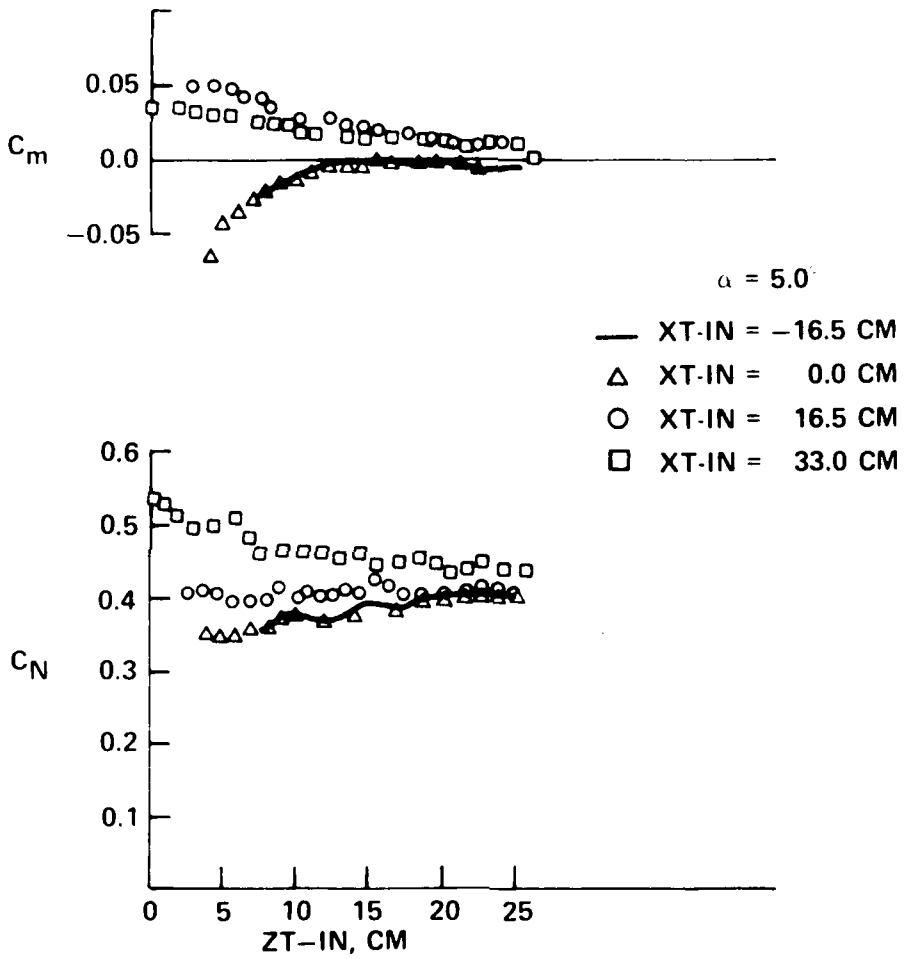

Figure 11 - Effect of Vertical and Longitudinal Locations on C_m and C_N

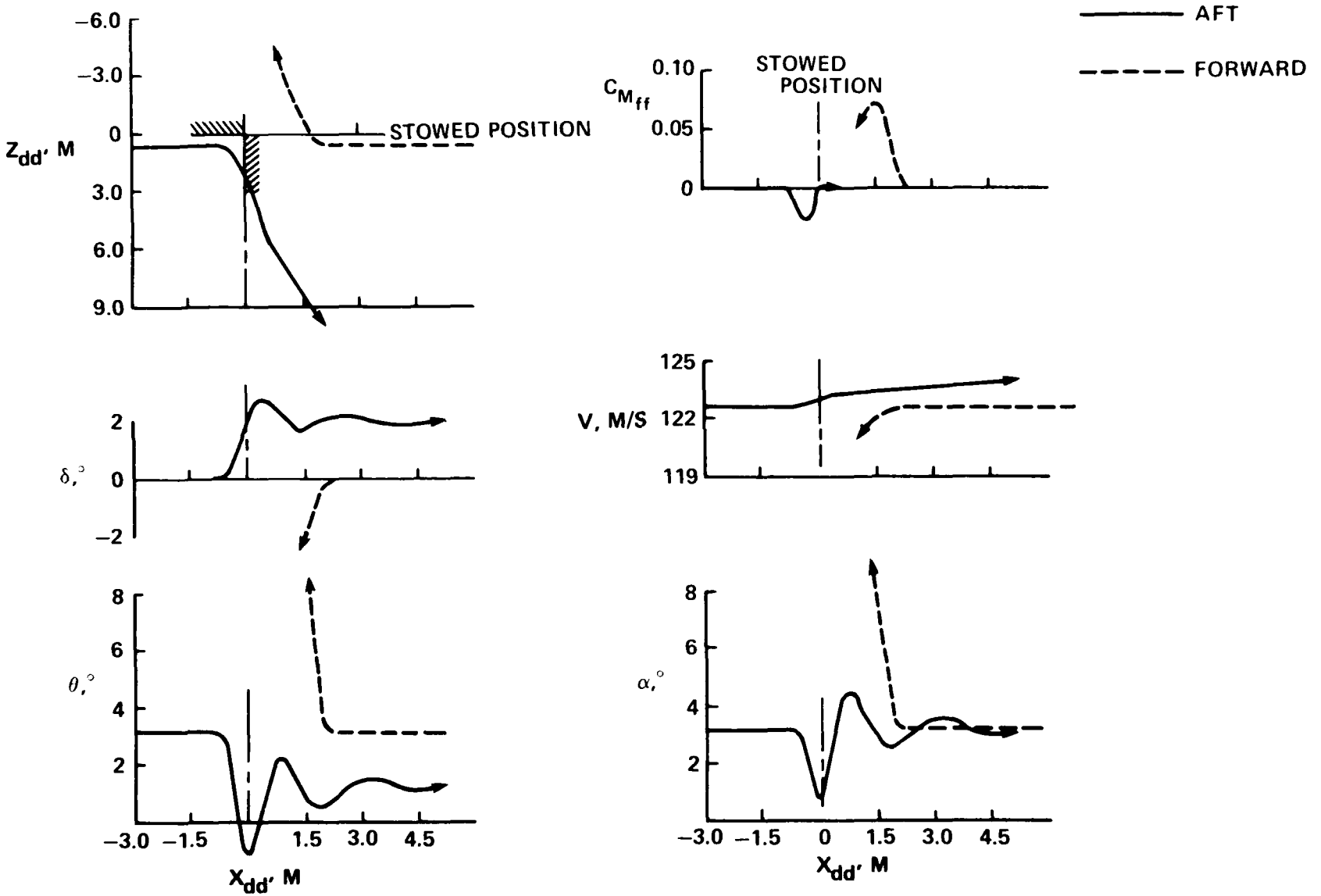

Figure 12 - Open-Loop Characteristics of the RPV for Aft and Forward Closure

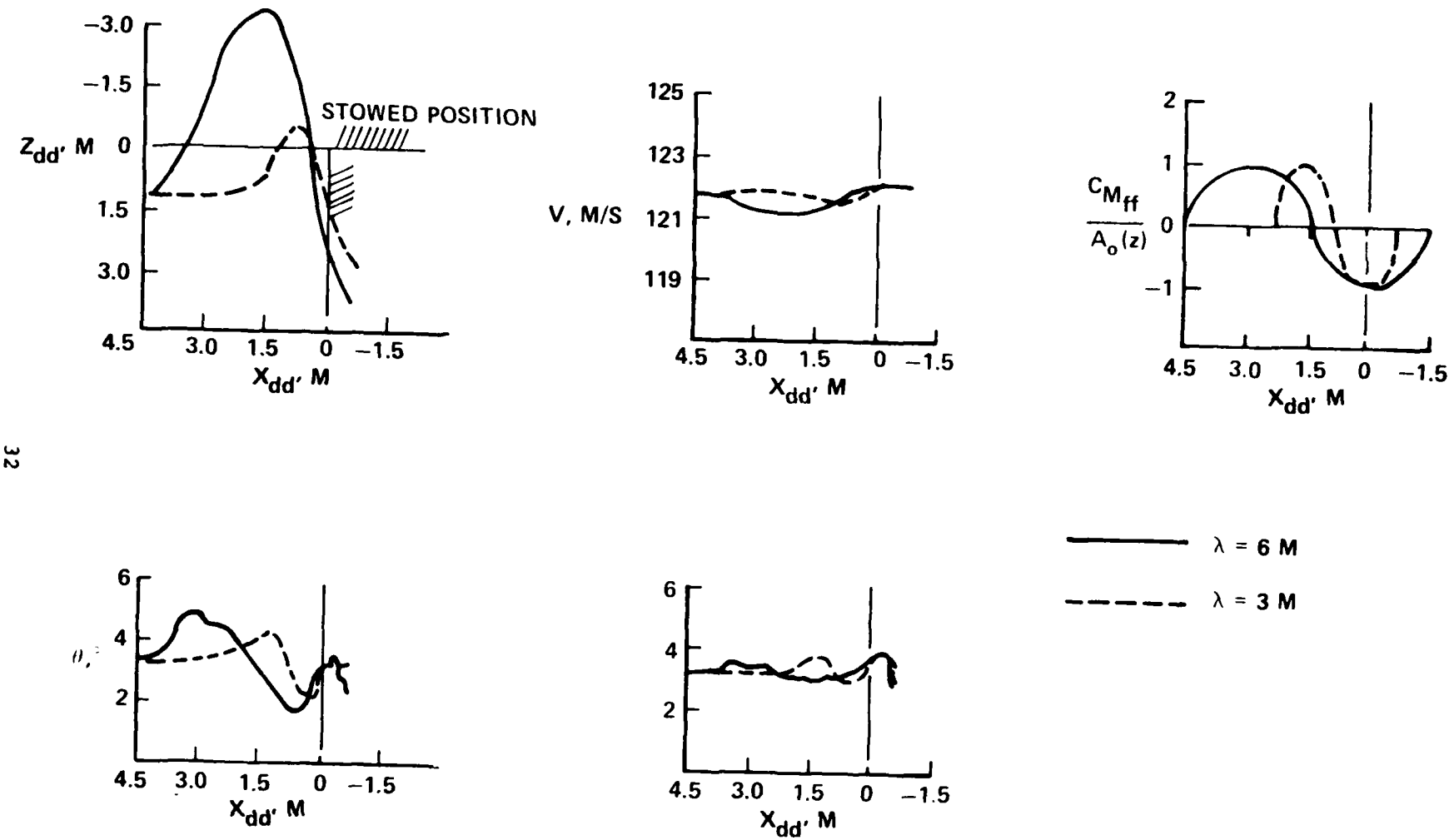

Figure 13 - Effect of Flow Field Wave Length on Forward Closure

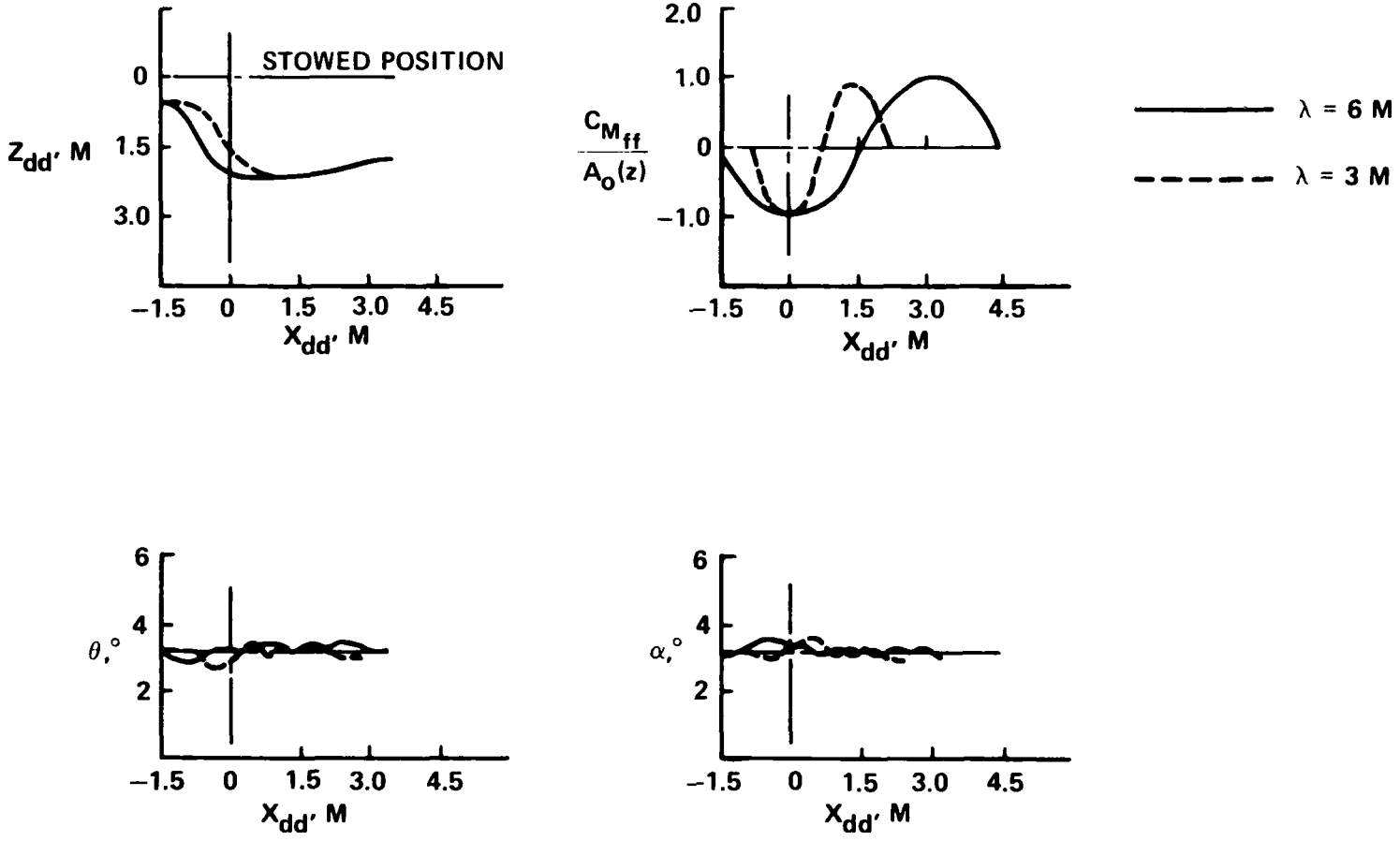

Figure 14 - Effect of Flow Field Wave Length on Aft Closure

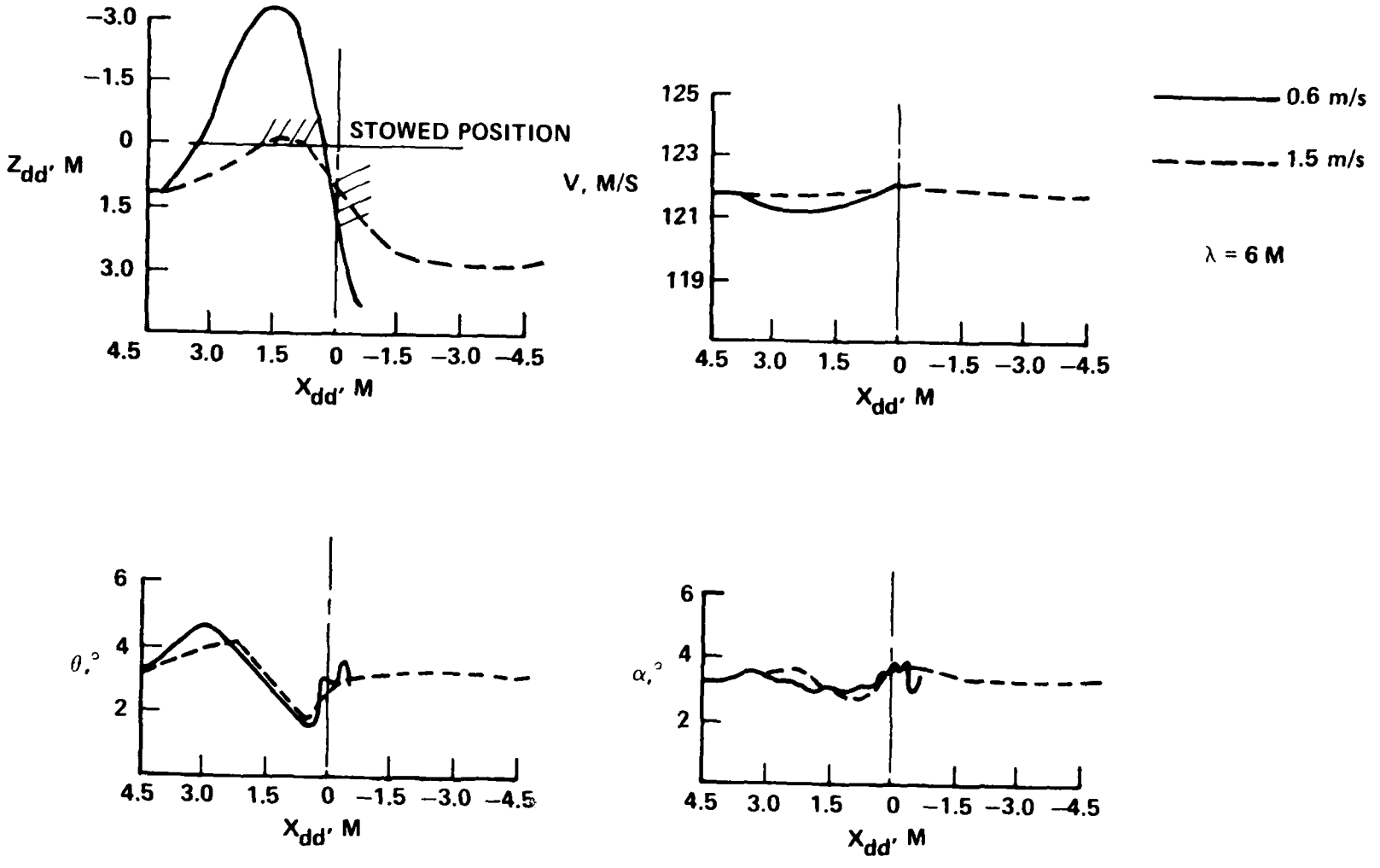

Figure 15 - Effect of Closure Rate on Forward Closure

INITIAL DISTRIBUTION

Copies	
2	CNO
	1 OP-506
	1 OP-508W
3	NAVAIRDEVCEN
	1 RPV Project Office (30P8)
	1 J. Wullert
	1 Tech Library
2	NAVWPNCEN
	1 R.E. Smith (4063)
	1 Tech Library
14	NAVAIRSYSCOM
	1 PMA 247
	1 PMA 235
	1 PMA 253
	1 AIR 03P25
	1 AIR 320
	1 AIR 510
	1 AIR 5102L
	1 AIR 5103F
	1 AIR 5301
	1 AIR 53011
	1 AIR 530113
	1 AIR 53012
	1 AIR 53013
	1 AIR 530313
2	PMTC
	1 G.F. Cooper (3152)
	1 Tech Library

CENTER DISTRIBUTION

Copies	Code
30	5214.1 Reports Distribution
1	522.1 Library (C)
1	522.2 Library (A)
2	522.3 Aerodynamics Library

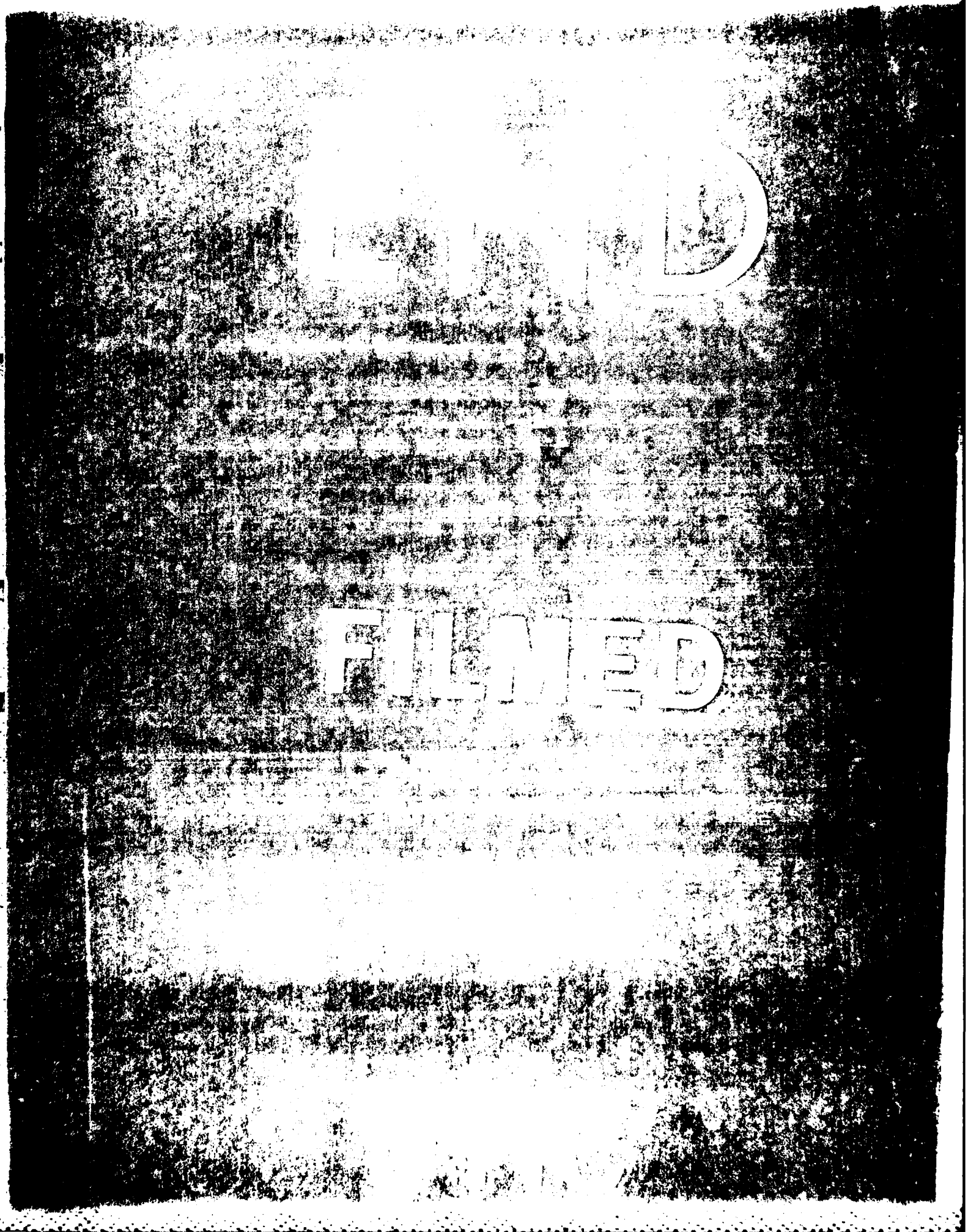
FILMED